NPP and N20 CrIS Full Spectral Resolution FOV Differences Derived from the NCEP GDAS.

James A. Jung[1], Agnes Lim[1], William McCarty[2], Yangrong Ling[3], and Mitchell D. Goldberg[4]

[1] CIMSS, Madison WI, [2] NASA/GSFC/GMAO, Greenbelt MD, [3]NOAA/NCEP/EMC/IMSG, Lanham MD, [4]NOAA/NESDIS/JPSS, Greenbelt MD.

Introduction

The Cross-track Infrared Sounder (CrIS) is a high spectral resolution Fourier Transform Spectrometer developed as a temperature and water vapor profiling instrument for weather forecasting. Its high accuracy also makes it suitable for climate applications. To use CrIS data in numerical weather prediction, it is important that its radiometric accuracy be understood. While several studies have looked at satellite inter-calibration (Goldberg et al., 2011, Chandler et al., 2013), few have addressed instrument field of view (FOV)-to-FOV differences (Gunshor et al., 2012, Strow et al., 2013, Tobin et al., 2013). As instruments improve, FOV-to-FOV differences become of greater concern to both Numerical Weather Prediction (NWP) and Climate studies.

Methodology and Design

A methodology for on-orbit adjustment of nonlinearity correction parameters to reduce the overall contribution to radiometric uncertainty and reduce the FOV-to-FOV variability of CrIS on Suomi National Polar-Orbiting Partnership (SNPP) and NOAA-20 is described in Tobin et al., 2013. To quantify the remaining FOV-to-FOV differences, a low resolution cycled version of the National Centers for Environmental Prediction (NCEP) Global Data Assimilation System (GDAS) is used. This system has a spectral resolution of T670 and uses a 4DenVAR technique. 80 ensemble members are used to derive the model background error statistics for the data assimilation step. The NCEP GDAS version used here is similar to the 2017 operational version and assimilated all non-restricted operational data. This baseline cycled assimilation also included the 431 subset CrIS from both SNPP and NOAA-20.

The FOV tests split off from the baseline cycled assimilation by using the 3-9 hour forecasts and the ensembles. All data were used by the baseline assimilation except CrIS. Quality control modifications specific to these experiments include; accepting clear profiles only over ocean, and accepting shortwave channels only at night. These quality control criteria reduce the errors associated with the radiative transfer model. The Gridpoint Statistical Interpolation (GSI) code was modified to accept data from only one CrIS FOV. The 2211 channel CrIS data went through all of the thinning and quality control procedures but were monitored instead of assimilated. The bias correction statistics for CrIS were removed at the start of the FOV experiments to allow statistics from each FOV to spin up independent of any previous FOVs. The bias corrections for each FOV adjusted based only on the specific FOV through the next 28 cycles (7 days).

The FOV experiments were conducted for 44 cycles (10 days) from 20180730 through 20180808. Bulk bias and standard deviation statistics were collected for each FOV. Assimilation statistics were monitored for any potential anomalies during this period. Channel statistics were consistent between channels and among the 9 FOVs.

References

Chandler, G., et al. (2013): Overview of inter-calibration of satellite instruments, *IEEE Trans. Geosci. Remote Sens.*, **51**, 1056-1080.

Goldberg, M., et al. (2011): The global space-based inter-calibration system, *Bull. Am. Meteorol. Soc.*, **92**, 467-475.

Gunshor, M., S. Moeller, and T. Schmit, 2012: Investigating the effects of detector-averaged SRFs, *NOAA Satellite Science Week*, Kansas City, MO, May 2012.

Strow, L., et al. 2013: Spectral calibration and validation of the Cross-track Infrared Sounder on the Suomi NPP satellite, *J. Geophys. Res. Atmos.*, **118**, 12486-12496.

Tobin, D., et al. 2013: Suomi-NPP CrIS radiometric calibration uncertainty. *J. Geophys. Res. Atmos.*, **118**, 10,589-10600.

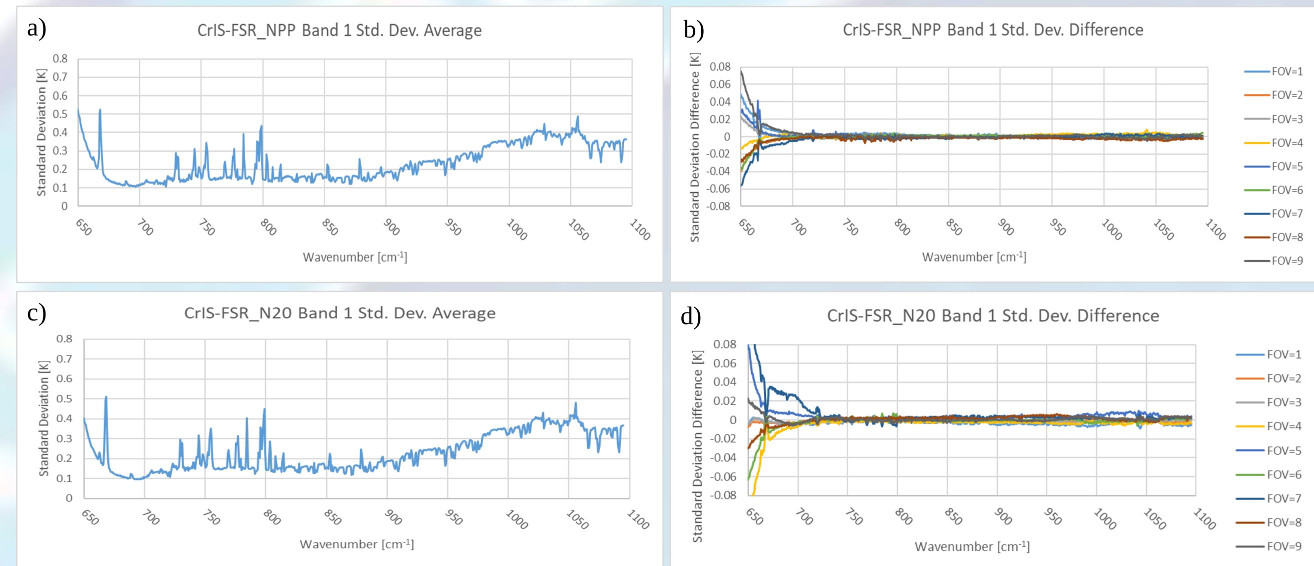

Figure 1: CrIS band 1 standard deviations. SNPP a) average of all FOVs and b) difference from mean of each FOV. NOAA-20 c) average of all FOVs and d) difference from mean of each FOV.

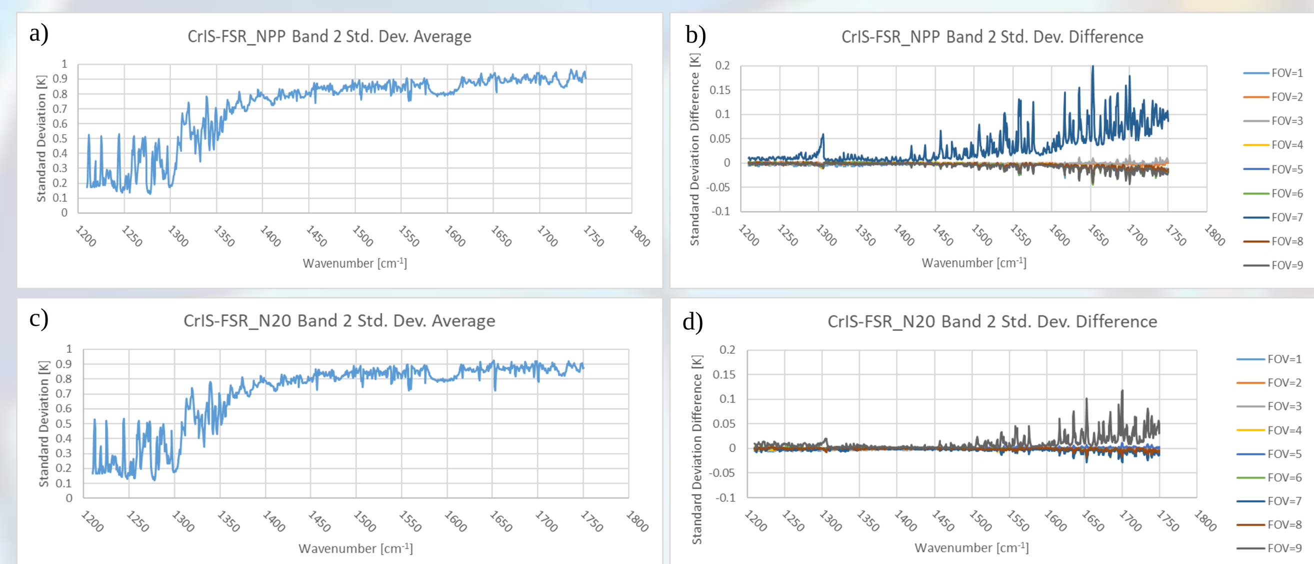

Figure 2: CrIS band 2 standard deviations. SNPP a) average of all FOVs and b) difference from mean of each FOV. NOAA-20 c) average of all FOVs and d) difference from mean of each FOV.

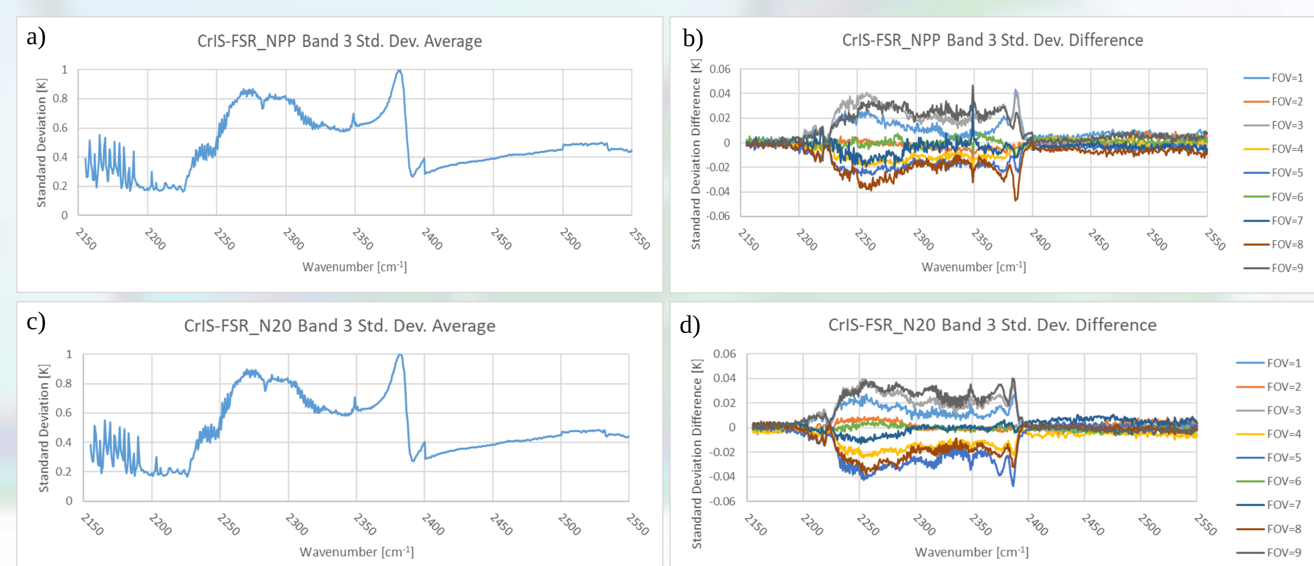

Figure 3: CrIS band 3 standard deviations. SNPP a) average of all FOVs and b) difference from mean of each FOV. NOAA-20 c) average of all FOVs and d) difference from mean of each FOV.

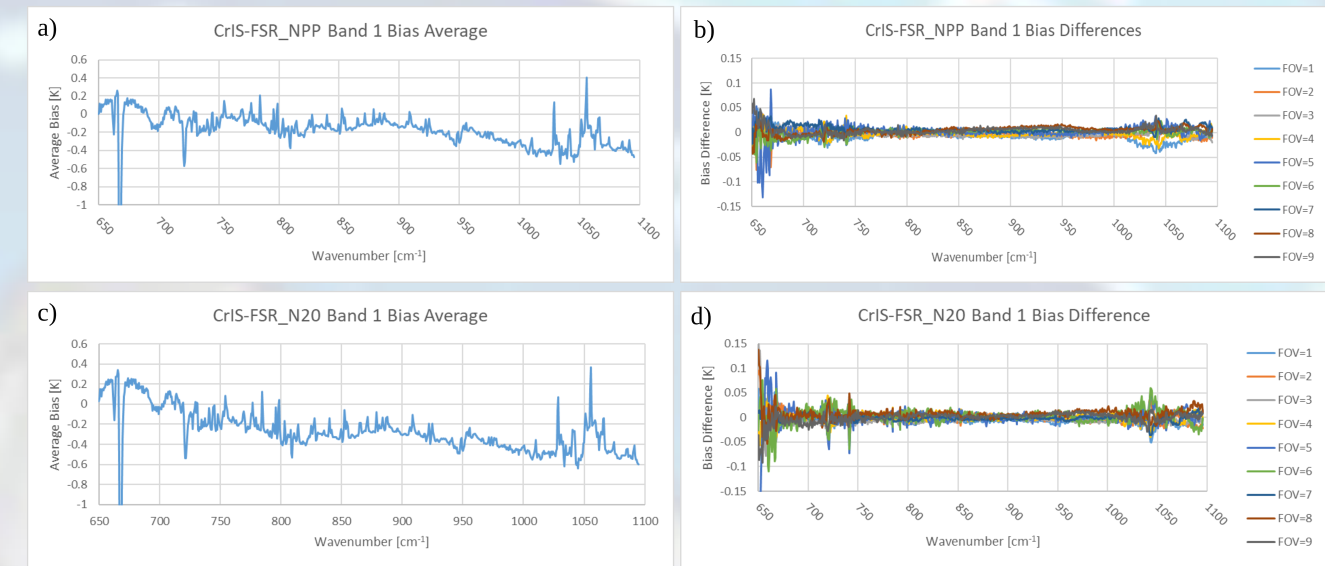

Figure 4: CrIS band 1 biases. SNPP a) average of all FOVs and b) difference from mean of each FOV. NOAA-20 c) average of all FOVs and d) difference from mean of each FOV.

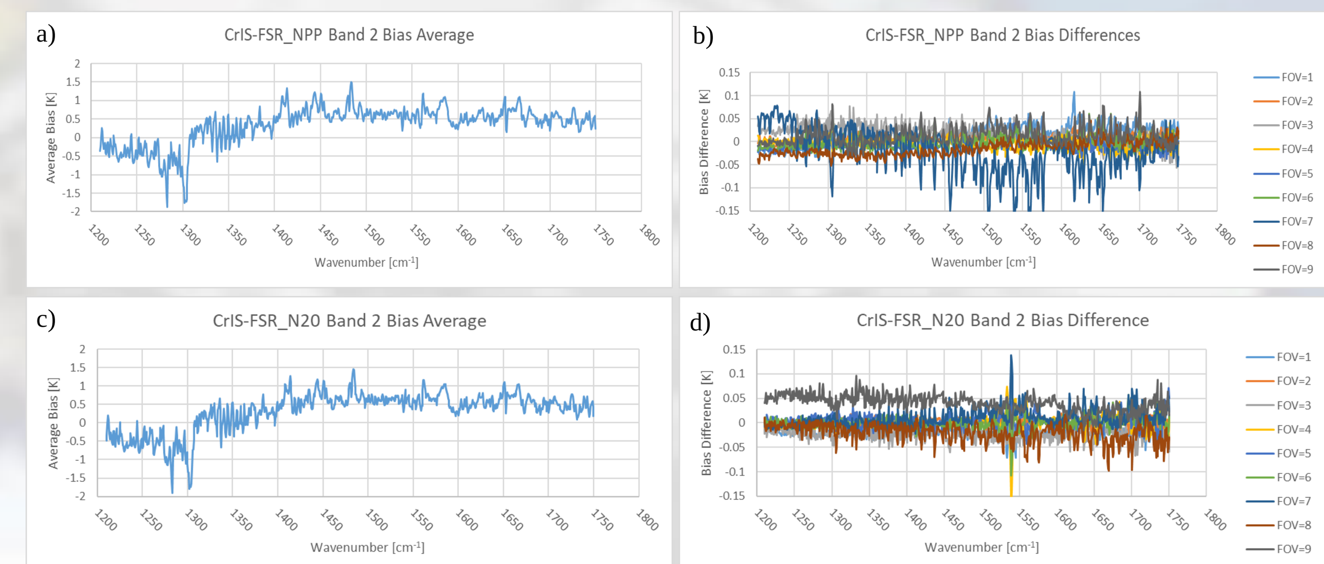

Figure 5: CrIS band 2 biases. SNPP a) average of all FOVs and b) difference from mean of each FOV. NOAA-20 c) average of all FOVs and d) difference from mean of each FOV.

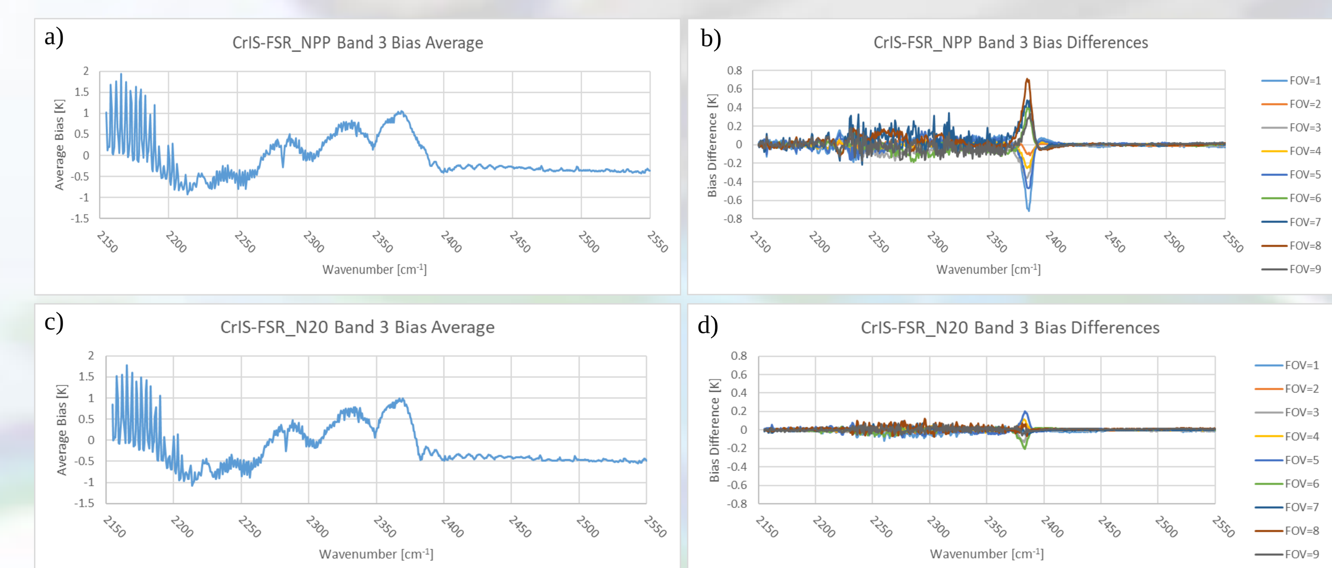

Figure 6: CrIS band 3 biases. SNPP a) average of all FOVs and b) difference from mean of each FOV. NOAA-20 c) average of all FOVs and d) difference from mean of each FOV.

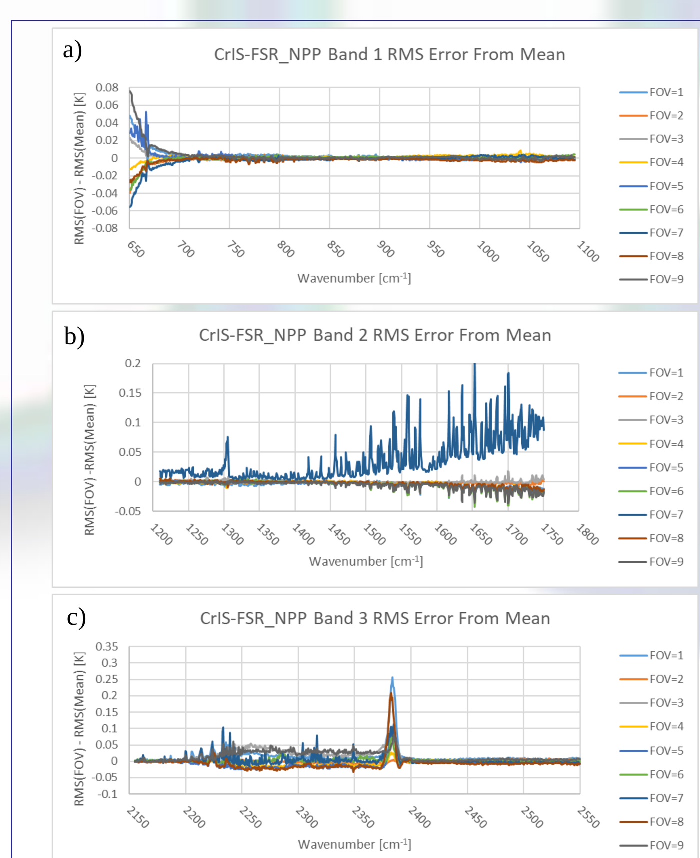

Figure 7: SNPP RMS differences. a) band 1, b) band 2 and c) band 3. FOVs with positive RMS values may require inflated observation errors during assimilation.

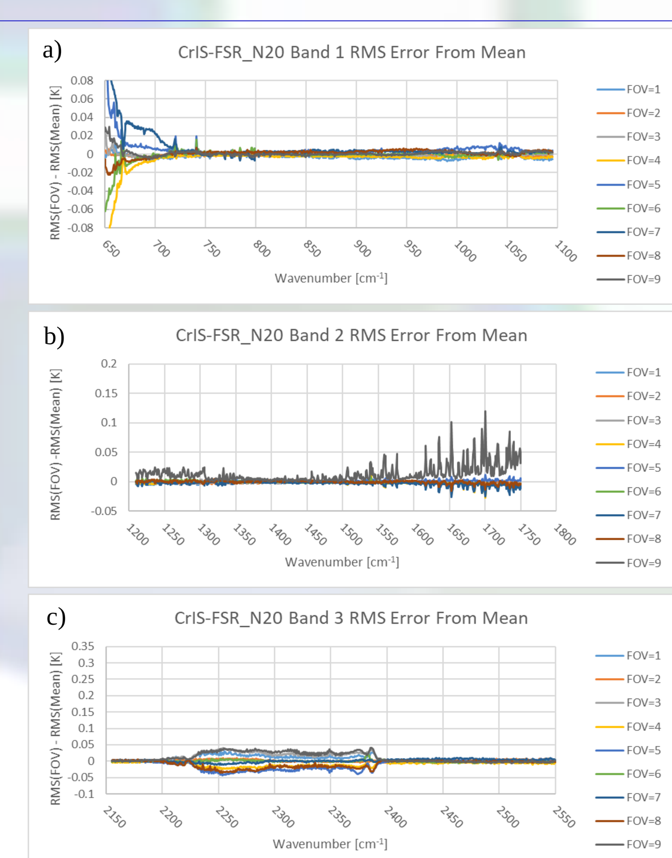

Figure 8: NOAA-20 RMS differences. a) band 1, b) band 2 and c) band 3. FOVs with positive RMS values may require inflated observation errors during assimilation.

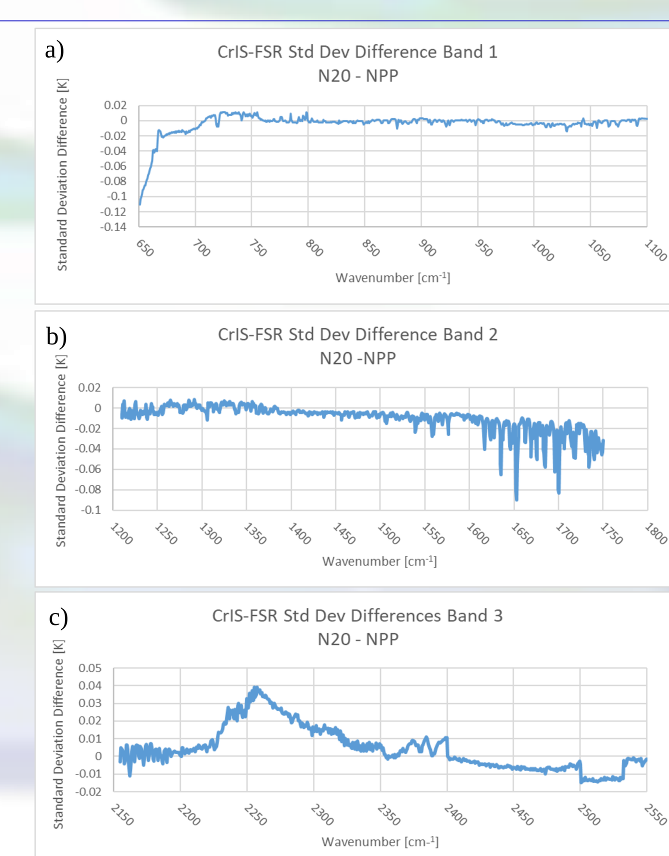

Figure 9: NOAA-20 – SNPP standard deviation differences. a) band 1, b) band 2 and c) band 3. Negative values indicate NOAA-20 has smaller average standard deviations.

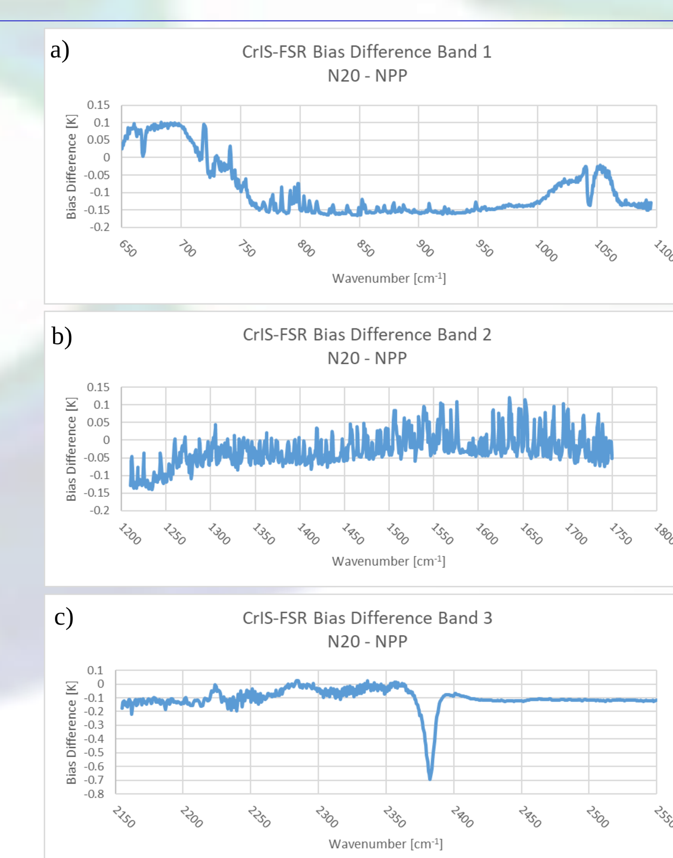

Figure 10: NOAA-20 – SNPP bias differences. a) band 1, b) band 2 and c) band 3. Negative values indicate NOAA-20 has smaller average bias.

Experiment Results

Standard deviation (σ) and bias statistics were derived from the GDAS analysis, averaged over all 44 cycles, then averaged over the 9 FOVs to determine the overall mean standard deviation and mean bias for SNPP and N20. The standard deviation statistics are shown in Figures 1, 2, and 3 for bands 1 (650-1095 cm^{-1}), 2 (1210-1750 cm^{-1}), and 3 (2155-2550 cm^{-1}) respectively. Statistics for SNPP are shown in panels a) and b) while statistics for N20 are shown in panels c) and d). Similarly, the bias statistics are shown in Figures 4, 5, and 6 for band 1, 2, and 3 respectively. The average of each FOV was then subtracted from the mean to determine FOV differences shown in panels b) and d).

Any bias differences between FOVs should be accounted for in the assimilation through the observation error. This is done by incorporating the FOV bias and standard deviation differences into the observation error. Since the mean bias is removed by the assimilation system, only the residuals from each FOV must be accounted for. The bias and standard deviation difference for each FOV is defined as:

$$\Delta bias_{v,fov} = bias_{v,fov} - bias_{v,mean} \quad (1)$$

$$\Delta\sigma_{v,fov} = \sigma_{v,fov} - \sigma_{v,mean} \quad (2)$$

The variance for each FOV becomes:

$$\sigma^2_{v,assim\_fov} = \Delta bias^2_{v,fov} + \sigma^2_{v,fov} \quad (3)$$

The observation error typically accounts for several errors including the representative error, forward model error, and instrument error. The other errors are assumed to be independent of the instrument error. The change in the instrument error for each FOV is:

$$\Delta\sigma_{v,assim\_fov} = \sigma_{v,assim\_fov} - \sigma_{v,mean} \quad (4)$$

The differences in instrument errors computed from (4) are shown in Figure 7 and 8 for SNPP and N20 respectively. The errors for band 1, 2, and 3 are in panels a), b), and c) respectively. Note: The standard deviation difference of a specific FOV may be smaller than the mean. An adjustment to the observation error based on the FOV may be necessary if the assimilation system uses statistics of the instrument instead of the FOV.

Conclusions

The FOV statistics shown here are consistent with the results from the CrIS SDR Team. FOV=5 of band 1 on SNPP has oscillations in the bias, FOV=7 of band 2 on SNPP is the most out of family. FOV=9 of band 2 on N20 is the most out of family. These FOVs also have the largest potential instrument errors.

The average bias and standard deviations differences (N20 – SNPP) are shown in figures 9 and 10 respectively for bands 1, 2, and 3. The differences in bias (Figure 9) are consistent with known differences between the two CrIS instruments (Larrabee Strow, personal communication). The differences in standard deviation are also consistent with the FOV averaged NEDN of both instruments.

The FOV standard deviation differences in band 3 (Figure 3 panels b) and d) are suspected to be from errors due to polarization and the source of future work.

Acknowledgements

Funding for this research was provided by the Joint Polar Satellite System through Cooperative Agreement grant NA15NES4320001. Computing resources were provided by the NASA Center for Climate Simulations.